IOP Conf. Series: Materials Science and Engineering **1302** (2024) 012006 doi:10.1088/1757-899X/1302/1/012006

Ultimate Tensile Strengths and Elastic Moduli at 20 K of Additively Manufactured PA840-GSL, A6061-RAM2, and AlSi10Mg

R Adams, G Rinauro, and J Leachman[1]

HYdrogen Properties for Energy Research (HYPER) Center, School of Mechanical and Materials Engineering, Washington State University, Pullman, WA, 99164-2920, USA

[1]Corresponding author. Email address: jacob.leachman@wsu.edu

Abstract. The additive manufacturing (AM) of polymer matrix composites (PMCs) and metal matrix composites (MMC) systems presents novel opportunities for reducing the mass of aerospace vehicles. These solutions also have the potential to reduce the cost of terrestrial applications where cryogenic temperatures are present. To address this need, this paper explores the mechanical characterization of three AM materials at 20 K: a nylon-based PMC PA840-GSL, and two aluminum-based MMCs A6061-RAM2 and AlSi10Mg. A Cryogenic Accelerated Fatigue Tester (CRAFT) used for the mechanical testing is first detailed. Next, ultimate tensile strengths and elastic moduli of the additively manufactured AlSi10Mg alloy and A6061-RAM2 are obtained. Third, the mechanical performance of an additively manufactured PMC liquid hydrogen tank constituent is collected in addition to an analysis on the effect the processing parameters, such as scan spacing, have on the mechanical behavior. A6061-RAM2 exhibited superior mechanical performance and is recommended for structural applications. Variation of PA840-GSL scan spacing resulted in decreased mechanical performance.

1. Introduction

AlSi10Mg alloy is commonly used in additive manufacturing as this material possesses a high mechanical strength and corrosion resistance (and easy to process via Laser-based AM). AlSi10Mg has the potential to be implemented in aerospace applications due to a low density. With cryogenic environments being characteristic of many aerospace applications, it is essential to identify the performance of this aluminum alloy at cryogenic temperatures. However, there currently exists a lack of material data on the AlSi10Mg alloy as mechanical testing of this additively manufactured alloy at 20K has never been performed.

Wide variability in aluminum AM material properties has been reported in the literature [1-3]. Li presents a study where selective laser melted (SLM) AlSi10Mg tensile properties are compared to those with an additional 1.0% by weight TiB_2. The addition of 1.0 weight percent ceramic resulted in the increase of ultimate tensile strength (UTS), yield strength (YS), and elongation by 9.73%, 64.4%, and 4.57% over the base alloy, respectively. The addition of the load-bearing ceramic improved the tensile strength, which presents a possible increase over AlSi10Mg. At room temperature, the thermal conductivity of 6061-T651 is 167 W/m-K, whereas additively manufactured AlSi10Mg is 103 ± 5 W/m-K and 119 ± 5 W/m-K for the XY and ZX print orientations, respectively. Although the thermal conductivity of 6061-T651 aluminum is greater than AlSi10Mg at room temperature, a parallel effort to this study found the cryogenic thermal conductivities to be significantly higher for AlSi10Mg. Due to these conflicting property trends, an A6061-RAM2 from Elementum 3D was selected as a material to compare with that of the AlSi10Mg tensile data at 20K.

The additively manufactured materials, AlSi10Mg and A6061-RAM2 did not have any mechanical data recorded at 20K. However, the 6061 aluminum with a T651 heat treatment has recorded mechanical data at 20K [4,5]. This Al6061-T651 was tested at room temperature to compare to the material data sheets provided by the material supplier [2]. This material was also tested at 20K to compare with what was found in the literature. Thereafter, a full mechanical analysis of the two AM materials allowed for a direct comparison in mechanical performance at 20K and promoted the use of A6061-RAM2 over AlSi10Mg in cryogenic applications. A matrix of tested sample configurations is provided in Table 1. Print orientation is labeled as XY to describe a single melted layer during printing whereas the ZX print orientation is perpendicular to a print layer. Figure 1 shows the print orientations.

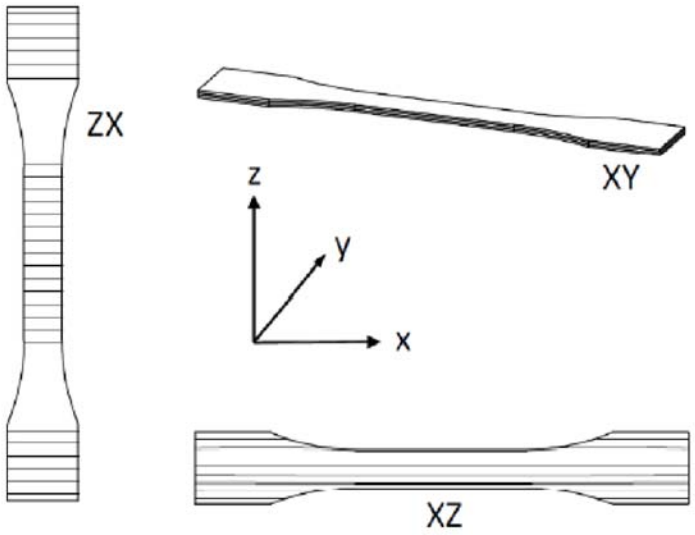

Figure 1. Conceptual schematic for print orientation.

Table 1. Sample Material Testing Matrix of the MMCs.

Material	Print Orientation	Temperature	Number of Tensile Tests
A6061-T651	N/A	RT	5
A6061-T651	N/A	20K	5
AlSi10Mg	XY	20K	5
AlSi10Mg	ZX	20K	5
A6061-RAM2	XY	20K	5
A6061-RAM2	ZX	20K	5

The 6061 aluminum with the T651 tempering aided in assuring data acquisition accuracy, whereas the two additively manufactured materials helped determine the relationship between print orientation and mechanical performance. The 6061-T651 aluminum samples were water jetted and machined to thickness from a 6.35 mm thick aluminum sheet with verified weight percent was 0.40-0.80% silicon, up to 0.7% iron, 0.15-0.40% copper, up to 0.15% manganese, 0.8-1.2% magnesium, 0.04-0.35% chromium, up to 0.25% zinc, up to 0.15% titanium, up to 0.15% other elements, and aluminum as the remainder [2].

AM polymer matrix composites (PMCs) present a unique opportunity for liquid cryogen fuel storage due to a shortened development lifecycle, reduced cost, and high specific strength. Additive manufacturing can reduce the time between initial concept and part implementation. Moreover, AM offers reduced costs for complex or low print quantity parts compared to traditional manufacturing methods. PMCs offer a unique trait in achieving the structural performance of metallics at a reduced mass. Greater than 60% of launch vehicle dry mass is attributed to the fuel and cryogenic tank [6]. Because this mass makes up a

majority of launch vehicle dry mass, higher specific strength alternative tank constituents have been proposed. Carbon fiber reinforced polymer (CFRP) cryogenic fuel tanks can offer mass savings between 20-40% by weight compared to aluminum alternatives [6]. This can reduce the mass required to store these liquid cryogens.

Samples were selective laser sintered by Northwest Rapid Manufacturing in an EOSINT P390 printer. A variety of design paths were selected to characterize the relationship between SLS process parameters and thermomechanical performance. To determine the range of parameters to be used for the design paths, the energy density in which the material melts and the energy density used for normal printing of the material had to be identified. Although the energy of melt for PA840-GSL was not made available, 0.290 J/mm^3 was identified as the energy of melt for a similar EOS alternative PA2200 (Nylon 12). The energy density used for the standard printing of the PA840-GSL material was identified to be 0.467 J/mm^3. Per ASTM D638, anisotropic materials require five samples to be tensile tested normal to and parallel with the principal axis [5]. To accommodate this requirement and ensure temperature-dependent strain compensation, ten samples were printed for each of four selected design paths. For each loaded sample there was an identical sample to serve as strain compensator during cooldown. The design paths feature two print orientations and two scan spacings that result in energy densities between the energy of melt and energy density commercially used in printing PA840-GSL. Table 2 shows the print settings for all four print configurations. It should be noted that only four samples were tested for the XY print orientation of the 0.27 mm scan spacing print configuration due to time constraints. Five tensile tests were performed for the other three print configurations. The processing chamber temperature and building platform temperature for all prints were 192°C and 160°C, respectively. The contours and edges of the prints utilized different laser speed and power parameters; laser speed was 1800 mm/s and laser power was 29.5 W exclusively for these features.

Table 2. Static Tensile Test Specimen Print Parameters of the PMC.

Print Orientation	Laser Speed (mm/s)	Laser Power (W)	Scan Spacing (mm)	Layer Height (mm)	Energy Density (J/mm^3)
XY	3600	29.5	0.27	0.1	0.381
ZX	3600	29.5	0.27	0.1	0.381
XY	3600	29.5	0.22	0.1	0.467
ZX	3600	29.5	0.22	0.1	0.467

2. Testing Methods

All tensile tests were performed in the Cryogenic Accelerated Fatigue Tester (CRAFT) at the Hydrogen Properties for Energy Research (HYPER) laboratory. Per ASTM D638 standard, tensile tests of anisotropic materials are required to test 5 specimens both parallel and normal to the principal axis [5]. These two print orientations were used to determine the relationship between print directions and corresponding mechanical performance. Given that the A6061-T651 was produced with conventional manufacturing, this directionality consideration does not apply.

All tensile testing was performed while referencing standard ASTM D638. Each specimen was manufactured with a type V geometry [5]. Measurements utilized a Starrett micrometer with a dimensional tolerance of +/- .002 mm. Each measurement was taken three times and averaged for the value utilized in calculating ultimate tensile strength and Young's modulus. Elastic modulus was calculated by the method of least squares. The coefficient of determination was 0.99 [7]. Utilizing the MTS TestSuite software, the test speed was set to 0.016 mm/s with stress and strain being populated in real time. A signal conditioner paired with the MTS software calculated the strain using a Vishay Micro-Measurements WK-13-125BZ-10C/W strain gauge, manufactured specifically for low-temperature applications, and mounted in the longitudinal direction on the gauge section of each sample. An additional sample accompanied each loaded sample to account for temperature-dependent strain during cooldown. This second sample was wired to the loaded sample and attached to the side of the grips in the test cell to compensate for temperature-dependent strain when cooling down. This can be seen in Figure 2.

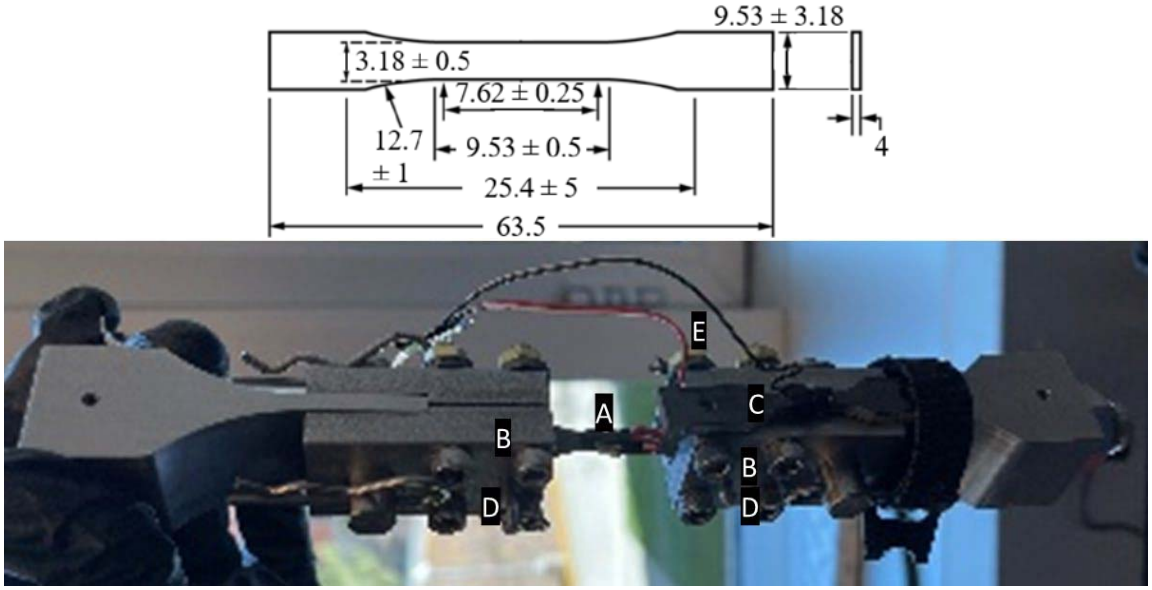

Figure 2. (Top) ASTM D638 Type V Sample Dimensions (mm) used for this study with holes drilled in each grip section to eliminate slippage. (Bottom) Specimen [A] mounted in CRAFT grips [B] assembly with the Compensating Specimen Configuration [C], slip pins [D], and temperature sensor [E].

Gauges were mounted in adjacent arms of the Wheatstone bridge configuration. Therefore, any voltage differential due to the temperature-dependent contraction of the sample at 20 K was negated. The gauge was then shunt calibrated at room temperature after installing the test cell and base plate and prior to pressurization of the test cell. This allowed for the proper correlation of zero force to zero strain. The test cell was pressurized with 2.7 bar of hydrogen, and the vacuum level achieved 1E-5 mBar prior to initiation of the cryocooler. The strain gauge was then shunt calibrated again due to an unequal force distribution attributed to test cell pressurization. The continuous hydrogen supply ensured the pressure was maintained at 2.7 bar during hydrogen liquefaction and the samples were tested in liquid hydrogen. During cooldown, the load frame was placed into force control mode to account for the contraction of components internal to the system. The specimens were allowed to thermally equilibrate overnight at 20 K before beginning the test. Prior to testing the strain gages were shunt calibrated for a third and final time to account for the temperature dependency of the strain gauge factor.

3. MMC Results

ASTM standard D638 was employed for all tensile testing. The ultimate tensile strength and elastic modulus are reported for each sample. The strain gauge's limit of ± 1.5% was exceeded for all tests, so no elongation data is reported herein. Upon the completion of data acquisition, standard deviation and standard error were calculated and recorded. Lateral failure within the gauge section was a commonality between all specimens. To validate accuracy of CRAFT data acquisition, the ultimate tensile strength and elastic modulus were obtained for the stock aluminum 6061-T651 samples at room temperature and 20K. This was then compared to data found in the literature and shown in Table 3.

At room temperature, the referenced UTS and Young's Modulus of the tested 6061-T651 aluminum was 310 MPa and 68.3 GPa, respectively [2]. The recorded ultimate tensile strength, 348 MPa maintained a 12.3% error from this expected value. The reported Young's modulus value for this material at room temperature, 69.45 GPa, had only 1.7% deviation from the reference value. At 20K, the UTS of 6061-T651 aluminum has been recorded as 497 ± 8 MPa, while the Young's modulus was 77.8 ± 0.78 GPa [4,8]. The tests performed at this temperature resulted in a recorded ultimate tensile strength of 535 MPa and a Young's modulus of 80.1 GPa. This resulted in a percent deviation of 7.6% for the ultimate tensile strength

and 3.0% for the Young's modulus. The reference ultimate tensile strengths at 20K and room temperature were not within the standard error of the measured values, but the reference Young's moduli are within the standard error of the measured values. This material's measured ultimate tensile strengths increased by 53.7% between room temperature and 20K, lower than the 60.3% percent increase between the referenced room temperature and 20K values. Moreover, the recorded Elastic Modulus of this material increased by 15.4% between room temperature and 20K, which was greater than the 13.9% increase observed between the referenced room temperature and 20K values. After these tests were completed, tensile testing of the additively manufactured AlSi10Mg and A6061-RAM2 were performed at room temperature and 20K. Table 4 illustrates the findings from these tests. The Literature Reference column includes the value recommended by NIST in the literature with the % error relative to these results. % Change is relative to manufacturers recommended values at room temperature.

Table 3. Recorded Elastic Modulus and Ultimate tensile strength of A6061 at Room Temperature (Top) and 20K (Bottom) Versus Reference Values.

A6061-T651 RT

Isotropic	Sample 1	2	3	4	5	Mean	Std Dev	Std Error	Literature Reference	% error
UTS (MPa)	332	337	366	355	351	348	14	6	310[a]	12.3
E (GPa)	56.7	74.6	83.9	60.6	71.5	69.5	10.93	4.89	68.30[a]	1.7

[a] *Test results did not support error bars on individual tests [2]*

A6061-T651 20K

Isotropic	Sample 1	2	3	4	5	Mean	Std Dev	Std Error	Literature Reference	% error
UTS (MPa)	549	495	562	553	517	535	28	13	497 ± 8[b]	7.6
E (GPa)	76.1	81.6	73.6	88.9	80.5	80.3	5.85	2.62	77.81 ± 0.78	3.0

[b] *Conservative calculation of error based on at least eight samples being tested [4]*

Table 4. Recorded Elastic Modulus and Ultimate tensile strength of A6061-RAM2 (Top) and AlSi10Mg (Bottom) Printed in the XY and ZX Print Orientations at 20K.

A6061-RAM2

Property	Print Direction	Sample 1	2	3	4	5	Mean	% Change	Std Dev	Std Error
UTS (MPa)	XY	532	627	564	552	564	568	71.6	36	16
UTS (MPa)	ZX	604	615	398	482	483	516	56.0	92	41
E (GPa)	XY	76.1	76.1	73.8	76.9	77.7	76.1	0.4	1.46	0.65
E (GPa)	ZX	78.7	71.9	87.5	78.0	73.0	77.8	2.6	6.18	2.76

AlSi10Mg

Property	Print Direction	Sample 1	2	3	4	5	Mean	% Change	Std Dev	Std Error
UTS (MPa)	XY	459	531	499	414	511	483	93.0	47	21
UTS (MPa)	ZX	449	457	465	511	678	512	104.7	96	43
E (GPa)	XY	73.4	70.6	90.3	61.3	72.0	73.5	1.0	10.51	4.70
E (GPa)	ZX	59.4	65.0	62.9	60.7	77.8	65.1	-10.5	7.39	3.30

The room temperature ultimate tensile strength of the MMC AlSi10Mg alloy has been reported to be 250 ± 11 MPa, while the Elastic Modulus of this material was identified as being 72.8 ± 1.1 GPa [10]. The room temperature UTS of A6061-RAM2 has been reported to be 331 ± 21 MPa, while the Young's modulus was reported as being 75.8 ± 0.7 GPa in both print directions [9]. Although additive manufacturing of these materials would result in anisotropic mechanical properties, no data were identified differentiating the mechanical properties in different print directions. Like the mechanical performance of these two materials at room temperature, results show that the ultimate tensile strength and Young's modulus of the A6061-RAM2 material are greater than the AlSi10Mg material at 20 K. At room temperature, the A6061-RAM2 maintains a 4.2% greater Young's modulus and 32.4% greater UTS compared to the AlSi10Mg. At 20 K, the differential in Young's modulus and UTS of these materials becomes 3.5% and 17.6%, respectively, for the XY-orientation and 19.5% and 0.8%, respectively for the ZX-orientation. A6061-RAM2 maintains substantially greater UTS and modulus data when compared to AlSi10Mg at 20K. It should also be noted that the XY-orientation A6061-RAM2 has the highest ultimate tensile strength at 568 MPa while the ZX-orientation of this material has the highest elastic modulus at 77.8 GPa. Compared to the 116 K data obtained of the A6061-RAM2 by Elementum 3D, the UTS at 20 K is 35.6% greater when considering the XY print orientation and 23.2% greater when considering the ZX print orientation.

4. PMC Results

All information required for the PMC by ASTM D638 was recorded for each test. Ultimate tensile strength, elastic modulus, and strain at break for each specimen are reported herein. Standard deviation and standard error were also calculated for the mechanical results obtained from each of the four print configurations. All specimens maintained lateral failure within the gauge section. For all data collected, the letter A represents a scan spacing of 0.22 mm and the letter B represents a scan spacing of 0.27 mm. The ultimate tensile strength of the PA840-GSL specimens tested are featured in Figure 3 below. No tabular results are presented due to the original measurement files being lost.

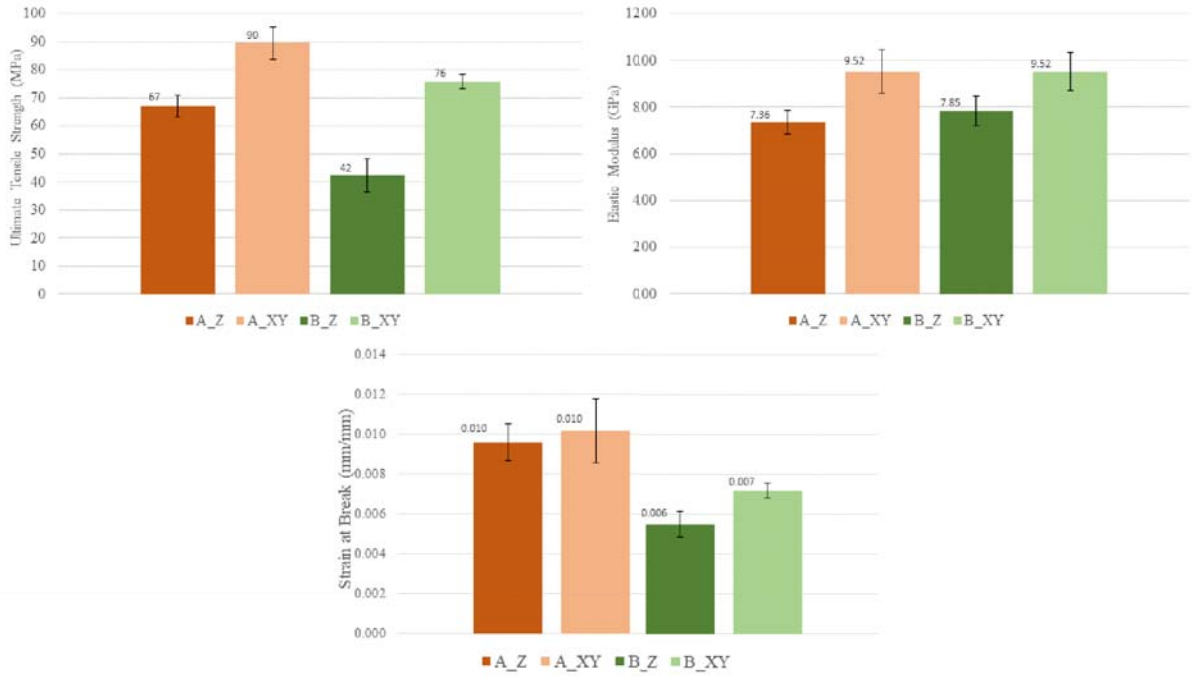

Figure 3. Ultimate tensile strengths, Elastic Moduli, and Strain at Break of PA840-GSL Tensile Specimens at 20K.

The XY-print orientation of all PMC scan spacing paths maintained a superior ultimate tensile strength at 20K compared to the ZX-print orientation counterpart. The XY print orientation of the 0.22 mm scan spacing had a 34.3% greater UTS than the ZX-print orientation and the XY print orientation of the 0.27 mm scan spacing had an 81.0% greater UTS than the ZX-print orientation. Between the 0.22 mm and 0.27 mm scan spacings, there was a 37.3% decrease and 15.6% decrease in UTS for the ZX print orientation and XY print orientation, respectively. The greatest UTS was observed by the 0.22 mm scan spacing of the XY print orientation with 90 MPa whereas the lowest UTS was observed by the 0.27 mm scan spacing of the ZX print orientation. The standard error of the data in the left panel of Figure 3 from left to right was 4 MPa, 6 MPa, 6 MPa, and 3 MPa.

Compared to the UTS, the difference in elastic moduli between the PMC scan spacings was not significant. The XY print orientations maintained greater elastic moduli overall. The elastic modulus of the 0.22 mm scan spacing XY print orientation was 29.3% greater than the modulus of the same scan spacings ZX print orientation. Similarly, the elastic modulus of the 0.27 mm scan spacing XY print orientation was 21.3% greater than the ZX print orientation of the same scan spacing. However, the difference between the elastic moduli of the 0.22 mm and 0.27 mm scan spacings in the same print orientations was negligible. The greatest elastic modulus observed was 9.52 GPa for both scan spacings of the XY print orientation whereas the lowest elastic modulus was 7.4 GPa for the 0.22 mm scan spacing of the ZX print orientation. The standard error for the elastic modulus data in the right panel of Figure 3 from left to right is 0.50 GPa, 0.93 GPa, 0.63 GPa, and 0.81 GPa.

Strain at break was low for all tests due to the extreme temperature-dependent embrittlement of the PMC at 20 K. The strain at break for the XY print orientations was found to be greater than the ZX print orientation samples. Between the ZX print orientation and XY print orientation of the 0.22 mm scan spacing, there was a 6% increase in strain at break. Between the ZX and XY print orientations of the 0.27 mm scan spacing, there was a 31% increase in the strain at break. The percent reduction in strain at break of the 0.22 mm and 0.27 mm scan spacing XY print orientations was 29%. The percent reduction in strain at break of the two different scan spacing ZX print orientations was 43%. The highest strain at break of 0.010 mm/mm was seen with the 0.22 mm scan spacing samples whereas the lowest strain at break of 0.006 mm/mm was seen with the ZX print orientation of the 0.27 mm scan spacing samples. The standard error for the data in the bottom panel of Figure 3 from left to right was 0.001 mm/mm, 0.002 mm/mm, 0.001 mm/mm, and 0.0004 mm/mm.

5. Conclusions

Mechanical property data of AM metallics and metal matrix composites are limited at cryogenic temperatures. The work conducted herein seeks to begin cataloging the performance of these AM metal-based materials at 20K. By performing tensile tests of the 6061-T651 material at room temperature and 20K, proof of accurate data acquisition was achieved for subsequent metallic testing. AlSi10Mg maintains significant tensile performance at 20K with ultimate tensile strengths of 483 MPa and 512 MPa for the XY and ZX print orientations, respectively and elastic moduli of 73.53 and 65.14 GPa for the XY and ZX print orientations, respectively. However, the A6061-RAM2 material has greater ultimate tensile strengths and elastic moduli in both print orientations. For Young's modulus, the A6061-RAM2 was 3.5% greater for the XY print orientation and 19.5% greater for the ZX orientation at 20K. Regarding UTS, the A6061-RAM2 was recorded as 17.6% greater for the XY print orientation and 0.8% greater for the ZX orientation at 20K. As such, it is recommended that A6061-RAM2 be utilized in applications where structural integrity is vital in response to applied loading.

The additively manufactured polymer matrix composite liquid hydrogen tank at the HYPER Center is composed of a PMC material with minimal mechanical performance data at 20K. Therefore, work was performed to characterize the mechanical performance of this material at 20K and to manipulate the processing of the tank to observe the change in mechanical performance. This modification has the potential to improve the thermal insulation of liquid cryogen fuel tanks which would permit the reduction of liquid cryogen boiloff. Upon the completion of tensile testing in CRAFT, it was found that the increase of scan spacing, and thereby reduction in energy density, had the potential to significantly reduce material tensile

performance. Future work should be done on manipulating AM processing parameters to cater to the performance of cryogenic applications in the future.

References

[1] Li, Yuxin, et al. “Effect of Trace Addition of Ceramic on Microstructure Development and Mechanical Properties of Selective Laser Melted AlSi10Mg Alloy.” Chinese Journal of Mechanical Engineering, vol. 33, 15 Apr. 2020, doi:10.1186/s10033-020-00448-0.
[2] Kaiser Aluminum Sheet Coil & Plate Alloy 6061 Technical Data Sheet
[3] EOS Aluminum AlSi10Mg Material Data Sheet
[4] Mann, D. LNG Materials & Fluids: A User's Manual of Property Data in Graphic Format. 1977.
[5] ASTM Standard D638, 2014, “Standard Test Method for Tensile Properties of Plastics," ASTM International, West Conshohocken, PA, 2014, DOI: 10.1520/D0638-14, www.astm.org
[6] Adam, Patrick Marshall, and Jacob W. Leachman. “Use of Nylon Blends for Lightweight Vapor Cooled Shielding of Liquid Hydrogen Fuel Tanks.” Washington State University, 2017.
[7] ASTM Standard E111, 2017, “Standard Test Method for Young’s Modulus, Tangent Modulus, and Chord Modulus," ASTM International, West Conshohocken, PA, 2017, DOI: 10.1520/E0111-04R10, www.astm.org
[8] Campbell, J. E., et al. “Handbook on Materials for Superconducting Machinery.” 1974.
[9] Elementum A6061-RAM2 Materials Data Sheet.
[10] McEnerney, Bryan W., et al. 2015, Qualification Methodology of AlSi10Mg for Spaceflight

Acknowledgements

This work was supported by the Department of Defense.